APPARATUS AND DEMONSTRATION NOTES

The downloaded PDF for any Note in this section contains all the Notes in this section.

John Essick, *Editor*
Department of Physics, Reed College, Portland, OR 97202

This department welcomes brief communications reporting new demonstrations, laboratory equipment, techniques, or materials of interest to teachers of physics. Notes on new applications of older apparatus, measurements supplementing data supplied by manufacturers, information which, while not new, is not generally known, procurement information, and news about apparatus under development may be suitable for publication in this section. Neither the *American Journal of Physics* nor the Editors assume responsibility for the correctness of the information presented.

Manuscripts should be submitted using the web-based system that can be accessed via the *American Journal of Physics* home page, http://ajp.dickinson.edu and will be forwarded to the ADN editor for consideration.

A compact grism spectrometer for small optical telescopes

Dominic A. Ludovici[a)] and Robert L. Mutel[b)]
Department of Physics and Astronomy, University of Iowa, Iowa City, Iowa 52242

(Received 15 December 2016; accepted 3 August 2017)

We describe a low-cost compact grism spectrometer for use with small astronomical telescopes. The system can be used with existing charge-coupled device (CCD) cameras and filter wheels. The optical design consists of two prisms, a transmission grating, a collimating lens, and a focusing lens, all enclosed in a 3D-printed housing. The system can be placed inline, typically in an unused filter wheel slot. Unlike conventional spectrometers, it does not require the target to be precisely positioned on a narrow slit. The mean resolving power ($R \approx 300$) is sufficient to resolve the spectral lines of many astronomical objects discussed in undergraduate astronomy labs, such as stellar absorption lines along the main-sequence, emission lines of early type hot stars and galactic novae, and redshifts of bright quasars and supernovae.
[http://dx.doi.org/10.1119/1.5000801]

I. INTRODUCTION

Many colleges and universities have on-campus observatories that are integrated into the undergraduate astronomy lab curriculum. These observatories are often equipped with sensitive, cooled CCD cameras that allow students to obtain impressive images of a wide variety of astronomical objects, including comets, planets, stars, nebulae, and galaxies. In contrast, however, spectroscopic observations dominate the observing schedules of most professional observatories. It is through the use of spectroscopy, in which light is separated into hundreds or thousands of spectral channels, that astronomers determine a large number of physical quantities that are either difficult or impossible to discern from an image. These quantities include chemical composition, temperature, density, motion (both translational and rotational), and even magnetic field strength.

To understand the results of astronomical research, it is critical for students to acquire experience in the use of spectroscopy.[1,2] For this purpose, low-resolution spectroscopic observations made with small telescopes can be used in undergraduate labs to determine physical laws and properties of many astronomical objects. For example, the wavelength of peak continuum intensity emitted by a blackbody (e.g., a star) allows one to infer the blackbody's surface temperature through Wien's law. The presence of absorption or emission lines indicates the presence of both atomic and molecular species and the relative temperatures of the emitting and intervening gases via Kirchhoff's laws. Doppler-shifted spectral lines can be used to study a wide variety of astrophysical phenomena, including stellar wind speeds, proper motions, and the expansion of the universe.

Despite the benefits of spectroscopic observations, relatively few small telescopes are capable of conducting such measurements. Small telescopes typically lack this capability because conventional spectrometers are expensive to build, very sensitive to vibration and temperature variations, and difficult to operate due to the fact that the target object must be placed on the spectrometer entrance with arcsecond accuracy. In addition, the spectrometer subsystem often interferes with CCD camera imaging or eyepiece observing, necessitating a cumbersome, time-consuming process of equipment removal and replacement whenever the spectroscope is installed. For these reasons, most spectroscopic observations in undergraduate astronomy labs have either used handheld spectroscopes for observations of terrestrial sources[1] or concentrated on collecting spectra of the Sun.[3]

While systems that permit telescopic observations of stellar spectra exist, they require the removal of the imaging equipment, are limited to observations of the brightest stars,[4] or produce low quality spectra.[5] A transmission grating placed directly in the optical path provides a simple low-cost way[5,6] to obtain low-resolution spectra with minimal equipment changes. This can be done by inserting the grating either into an eyepiece for visual observing[7] or in a filter wheel using the existing imaging camera as a detector.[8,9]

However, the dispersed spectrum suffers from an optical aberration, which severely limits the spectral resolution: The dispersed spectrum focuses on a curved surface rather than a flat plane (Petzval field curvature[10]). This limits the effective resolving power of simple transmission gratings to $R \equiv \lambda/\Delta\lambda \lesssim 100$ over the visible wavelength range.

Grism spectrometers,[11] which combine a transmission grating with a prism, minimize field curvature aberration by redirecting the dispersed rays closer to the optical axis. These systems can be used in large focal ratio ("slow") optical systems without additional corrective optics since the incoming rays are close to paraxial (e.g., the Hubble Space Telescope WFC3 grism[12]). However, most small observatory telescopes have fast optics (f/5-f/10), and so, the incident rays are significantly non-paraxial. In order to eliminate the coma and astigmatism produced by a wedge prism placed in a converging beam,[13] corrective optics must be used to collimate the incident rays and refocus the exit rays onto the image plane.

Here, we describe a low-cost, compact grism system with corrective optics that can be constructed using commercial off-the-shelf optical components. It is small enough to fit into existing commercial filter wheels with the addition of a small housing extender. The grism enclosure and filter wheel extension are easily fabricated using a 3D printer. The resolving power ($R \sim 300$) is sufficient to observe targets demonstrating a wide range of astrophysical phenomena, such as stellar spectral types, emission lines from hot star and novae, and redshifts of bright quasars and Type II supernovae.

II. THE COMPACT GRISM SPECTROMETER

A. Optical design

The compact grism spectrometer (CGS) optical design consists of five elements: A transmission grating, two achromatic lenses for collimating and refocusing, and two wedge prisms. In principle, a single prism can be used, but a typical grism design requires a large ($\theta \sim 20°$) prism refraction angle, which is not commercially available as a stock item. Figure 1 shows a ray trace of the optical design.

We now consider the design criteria for each element.

- **Diameter of optical elements.** Achromatic lenses, transmission gratings, and wedge prisms are commonly available[14–16] in both 25 mm and 50 mm sizes. For a compact design and to minimize weight, 25 mm diameter components are preferable. However, to avoid vignetting, the lens' clear aperture must be larger than the beam size δx at the grism

$$\delta x = d/\mathrm{f} < 25\,\mathrm{mm},$$

  where d is the distance from the grism to the focal plane and f is the focal ratio (= lens' focal length/aperture).
- **Collimating lens.** The collimating lens corrects for the converging telescope beam, creating a parallel beam. The lens is a negative (diverging) achromatic lens whose focal ratio is chosen to collimate the converging rays from the telescope optics. The exact focal length depends on where the lens is placed in the optical path. For a fully illuminated lens, an f/6.8 telescope beam can be collimated with a 25 mm diameter achromatic lens with a focal length $f = -170$ mm. However, for a partially illuminated lens (i.e., closer to the focal plane), the (negative) focal length increases.

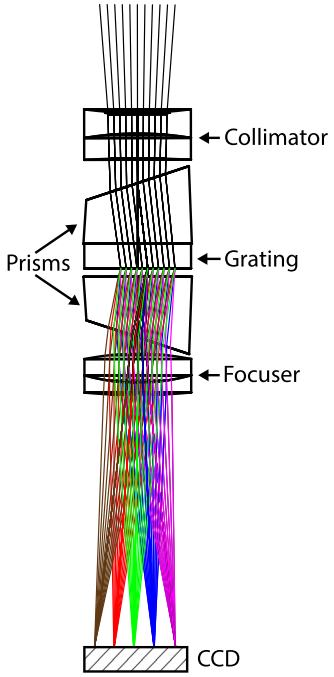

Fig. 1. Optical design of the compact grism spectrometer, showing ray paths at several wavelengths from 400 nm (magenta) to 800 nm (brown). The incident rays from the telescope (f/6.8) are first collimated by an achromatic doublet lens, then dispersed by a 10° wedge prism, followed by a 600 lpmm transmission grating, then a second 10° prism, and finally refocused into the detector plane by a second achromatic doublet. The focal lengths of the collimating and refocusing lenses are determined by the f-ratio, location in the converging optical beam, and the back-spacing of the imaging sensor.

- **Wedge prism.** The wedge prism compensates for the wavelength-dependent dispersion angle of the grating. The prism refraction angle, which is nearly wavelength-independent, is chosen to redirect the center wavelength of the observed spectrum back onto the optical axis. For example, for a 600 lines per millimeter (lpmm) grating and a center wavelength of 550 nm, the grating dispersion angle is 19°. Commercially available stock wedge prisms[15] range from 2° to 10° in 2° increments, so we chose to use two 10° prisms.
- **Transmission grating.** Stock transmission gratings range from 300 to 1200 lpmm groove spacing, with larger values providing increased spectral resolution, but at lower efficiency. Also, higher resolution gratings require larger wedge prism refraction angles and larger sensor sizes. In order to cover a wavelength range $\Delta\lambda$, a sensor located a distance d from a grating with groove spacing $a = 1/\mathrm{lpmm}$ must have a minimum linear dimension D_s of

$$D_s = \frac{\Delta\lambda}{a} d.$$

  For the full visible wavelength range $\Delta\lambda = 300$ nm, $d \sim 50$ mm, and a 600 lpmm grating ($a = 1.67\mu$), the sensor size must be at least 9.4 mm. While a holographic grating on a plastic substrate could be used, maximum efficiency of the system is obtained using a blazed grating on a glass substrate.
- **Refocusing lens.** The refocusing lens is a positive achromat, with a focal length approximately equal to the physical distance from the grating to the focal plane (sensor). For a two prism system, such as described here, the

distance is somewhat smaller, since the second prism lies between the grating and the refocusing lens.

We have found that both the collimating lens and refocusing lens focal lengths do not need to be exactly matched to the telescope focal ratio and sensor back focus, since a small change in telescope focus can compensate for the optical path difference.

- **Enclosure.** The optical elements are housed in a plastic enclosure fabricated using a 3D printer. Figure 2 shows the CGS in its enclosure and its installation in the filter wheel. Figure 3 shows an engineering drawing of the CGS enclosure and optics used on the Iowa Robotic Telescope. For most commercial filter wheels, an enclosure extension is required to allow adequate clearance for the grism, as illustrated in Fig. 4. This can be inexpensively printed using a 3D printer. Index marks included on the 3D-printed component indicate the dispersion direction of the grating. These marks can be positioned perpendicular to a line running from the center of the filter wheel to the grism, allowing easy alignment of the dispersed spectrum with the rows or columns of the camera CCD.

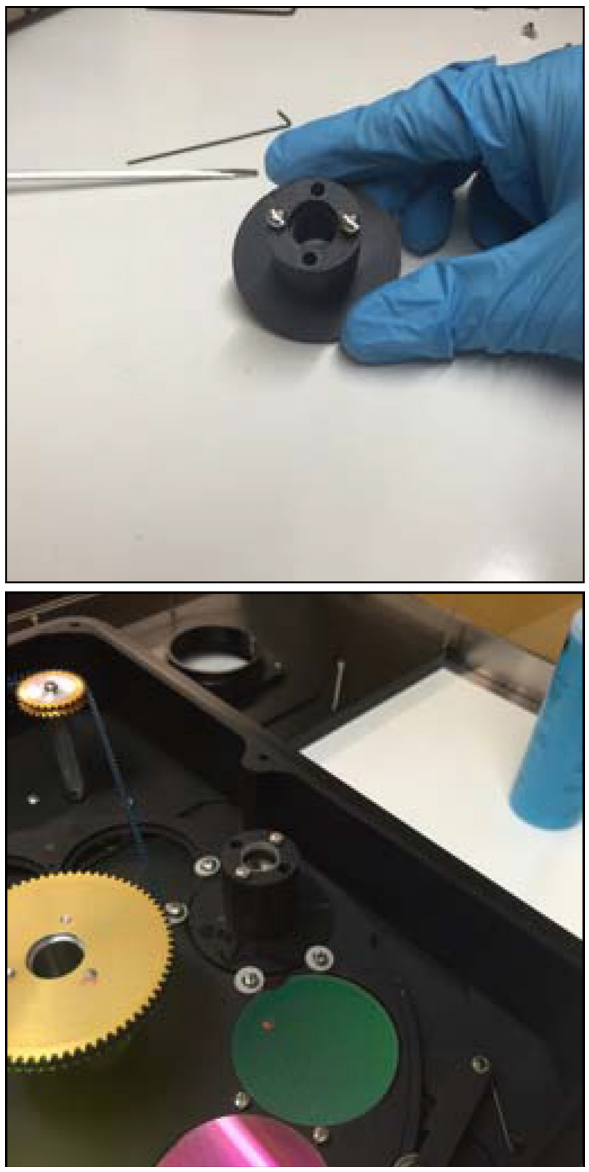

Fig. 2. [top] Compact grism system, with 25 mm optical components, enclosed in a 3D-printed housing. [bottom] Compact grism installed in a 50 mm diameter slot in a filter wheel. Note that the filter wheel housing has a 3D-printed wall extension with a height of 37 mm.

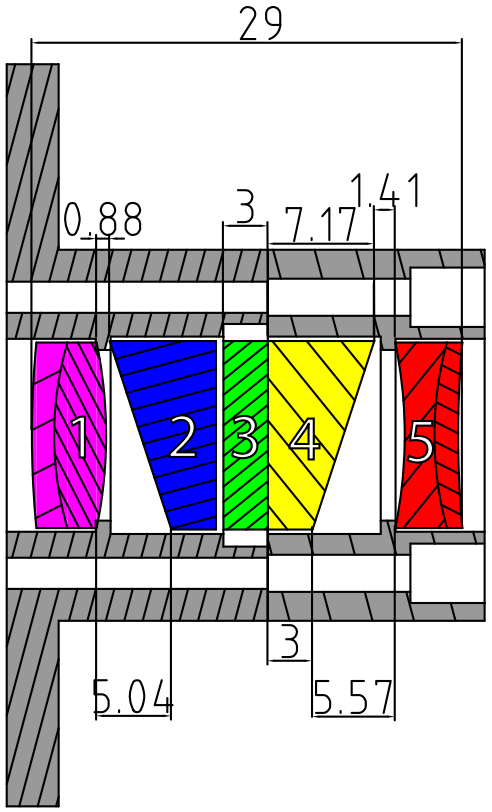

Fig. 3. Engineering drawing of the Compact Grism System (CGS). In this example, the system uses 25 mm optical components. The collimating lens (5) has a focal length of −75 mm and the focusing lens (1) has a focal length of +50 mm. The wedge prisms (2,4) have a 10° beam deviation. The grating used is a 600 lpmm blazed grating (3). All optical components are enclosed in a 3D-printed housing (gray). Sizes shown are in millimeter.

B. Wavelength and flux calibration

An example of a raw dispersed spectrum recorded on the imaging camera is shown in Fig. 5. In order to obtain an astronomically useful spectrum, the raw image requires both CCD and spectral calibration. The CCD calibration, consisting of thermal and bias subtraction as well as cosmic ray removal, is a standard procedure for CCD imaging at most observatories and will not be discussed here. Note that a flat field correction, which is normally applied to images, is not

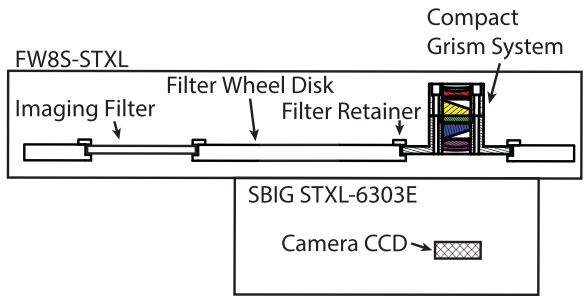

Fig. 4. Cross-sectional view of a filter wheel with the grism installed.

Fig. 5. Dispersed grism spectrum zero-order with stellar image at left. The image is focused at the center of the dispersed spectrum so that the stellar image is strongly defocused.

needed for spectroscopic observations since the gain variations across the dispersed spectrum are corrected by gain calibration, as described below.

Spectral calibration has two components: Wavelength calibration and flux calibration. The wavelength calibration is done in two steps. First, the target star is observed with a broadband filter. Small pointing offsets are then applied to place the object exactly at the field center. This adjustment can be done either manually or by solving for the center coordinates using an astrometric image solver (e.g., Pinpoint[17]). After this recentering, the grism image is taken and major spectral features (e.g., the Balmer sequence for an A-type star) are matched with corresponding pixel values. The wavelength-pixel data are fit with a low-order polynomial, and the corresponding coefficients are stored in a configuration file.

The flux calibration, which corrects for wavelength-dependent efficiencies in the imaging sensor, transmission grating, and telescope optics, can be determined by comparing raw spectra with flux-calibrated spectra of standard stars taken at a comparable spectral resolution and wavelength range. Fortunately, these are readily available in a downloadable form[18,19] and were used to calculate a table of gain coefficients for each spectral channel. Figure 6 shows an example of a raw spectrum and wavelength-flux calibrated spectrum.

III. SAMPLE CGS SPECTRA AND LAB PROJECTS

The grism spectrometer is installed at the Iowa Robotic Observatory,[20] a 0.5 m diameter f/6.8 Cassegrain reflector located at the Winer Observatory,[21] about 80 km SE of Tucson AZ, and operated from campus at the University of Iowa in Iowa City. The imaging system consists of a 2048×2048 format 13.5 μm pixel back-illuminated CCD camera equipped and a 12-position filter wheel, where one slot contains the CGS. This system is used by students and faculty at the University of Iowa for teaching and research. It is typically operated robotically using a queued observing list but can also be operated in real time using a high-speed Internet connection. When operated in the robotic mode, the wavelength calibration has a RMS error of $\sim$1 nm due to uncertainties in the telescope pointing.

A few examples of grism observing projects that have been done in undergraduate laboratories are shown below. They illustrate the range of astronomical objects that can be investigated spectroscopically.

- Figure 7 shows a sequence of four stellar spectra from very hot to very cool stars, with surface temperatures ranging from 19,000 to 3400 K. The spectra illustrate how the hydrogen Balmer lines become dominant near spectral type A and then rapidly decrease for solar-type stars, with molecular metal band dominating the coolest stars. These spectra were used by the students to investigate stellar temperatures using Wien's law. Interpreting these spectra also requires students to apply Kirchhoff's laws because the absorption lines are created by a blackbody spectrum passing through cooler gas. For more advanced students, the change in strength and equivalent width of the Balmer lines as a function of stellar temperature can be used to

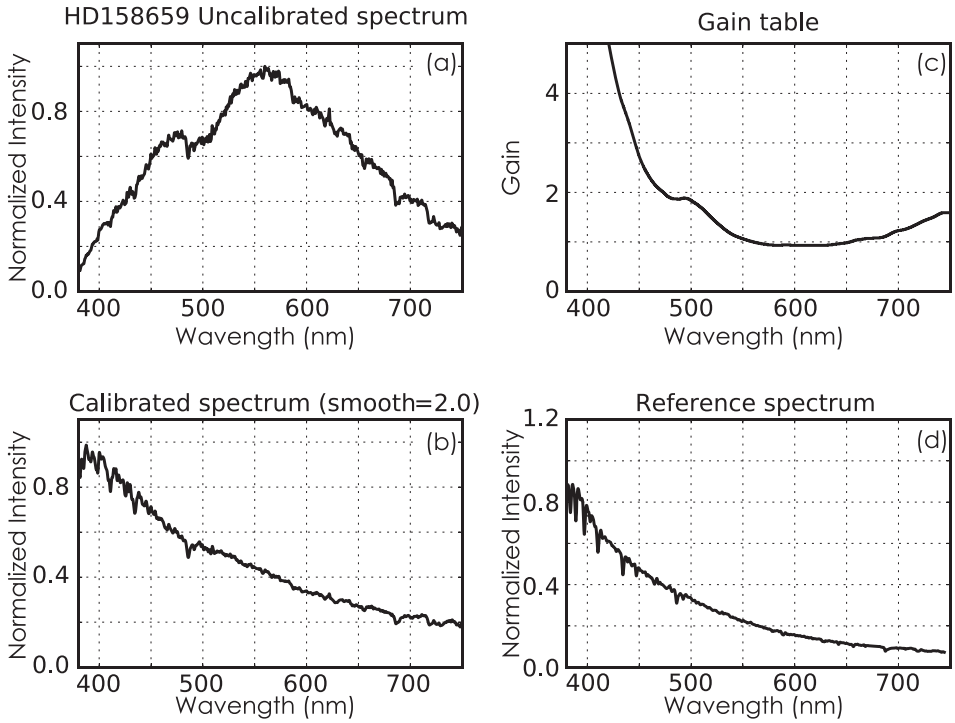

Fig. 6. (a) Uncalibrated spectrum of the B3V star HD158659. (b) Calibrated spectrum, (c) Gain curve applied to raw fluxes. (d) Calibrated spectrum of HD158659 from Jacoby *et al*. (Ref. 18).

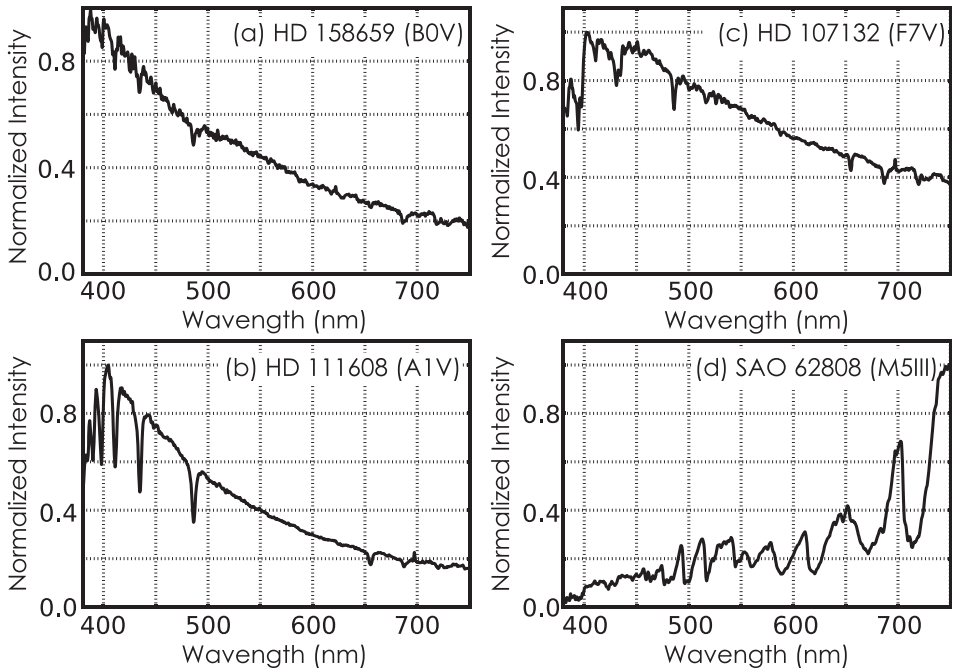

Fig. 7. Grism spectra of stars from 380 to 750 nm, illustrating the spectral sequence from hot to cool stars: (a) B3V:19,000 K (b) A1V: 9000 K, (c) F7V: 6240 K, and (d) M5III: 3400 K.

show the observational consequences of the Boltzmann and Saha equations.

- Figure 8 shows the spectrum of an emission-line star, in which circumstellar gas is heated in the chromosphere or in a disk by rapid rotation. This hotter gas produces emission lines at longer wavelengths where the gas is optically thick; at shorter wavelengths, one sees absorption lines arising from the photosphere. As with the example above, students can use emission line stars such as HD76868 to investigate Kirchhoff's laws.

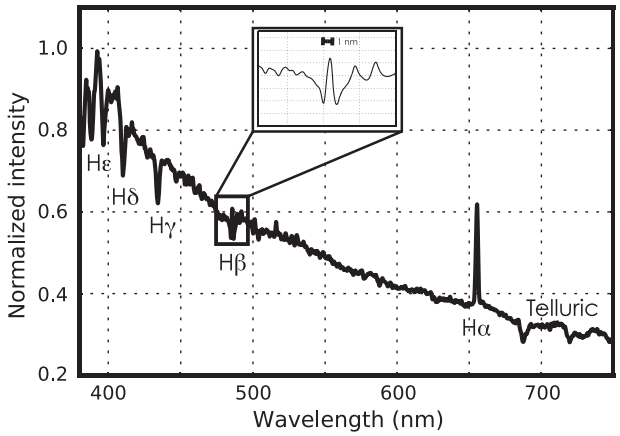

Fig. 8. CGS spectrum of the emission-line star HD76868 (B5e). Note the prominent chromospheric Hα emission line, which arises from circumstellar material ejected by the rapid rotation of the star. The circumstellar gas is optically thick in the Hα line, but with increasing frequency it becomes optically thin and the higher level Balmer lines are seen in absorption. The Hβ line has both emission and absorption components. The width of the emission component is $\Delta\lambda \sim 0.9$ nm, indicating a resolving power $R \approx 300$. Students examining these data will notice that the emission lines are narrower than the absorption lines. The emission lines form in the stellar wind, further away from the star. The emission lines are narrower because the effects of collisional broadening are lessened due to lower density in this region.

- Figure 9 shows the spectrum of WR7, an extremely luminous (280,000 $\times L_{sun}$) star with a chemically enriched high-speed wind whose emission lines dominate the spectrum. The widths of the spectral lines are dominated by Doppler broadening ($\Delta\lambda \approx 2$ nm) and are spectrally resolved by the CGS. Students in a laboratory setting can use the Doppler formula to measure wind speeds of several thousand kilometer per second in these stars.
- Figure 10 shows the spectrum of two bright (apparent visual magnitude $V = 14.4, 12.9$) quasars whose redshifts are readily obtained from the prominent Hα emission lines, which are displaced from the rest wavelength of 656.3 nm due to the Doppler effect. In addition to several other Balmer lines, both spectra also show prominent forbidden-line emission of doubly ionized oxygen III [OIII] arising from the narrowband region of the quasar. Students observing these objects in lab can measure the

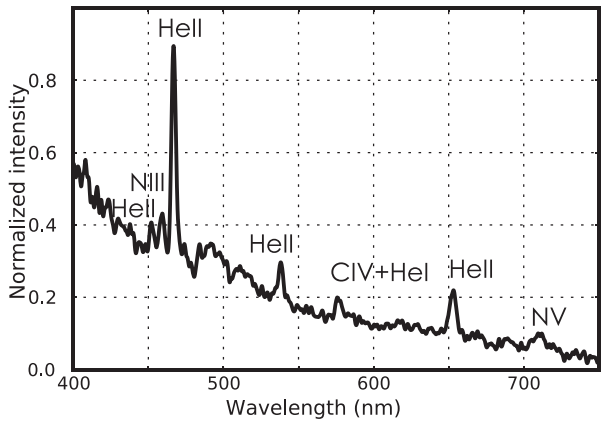

Fig. 9. CGS spectrum of the extremely luminous Wolf-Rayet star WR7 (HD56925) at the center of the emission nebula NGC2359. This star has an extended hot wind responsible for the broad emission lines of helium, carbon, and nitrogen.

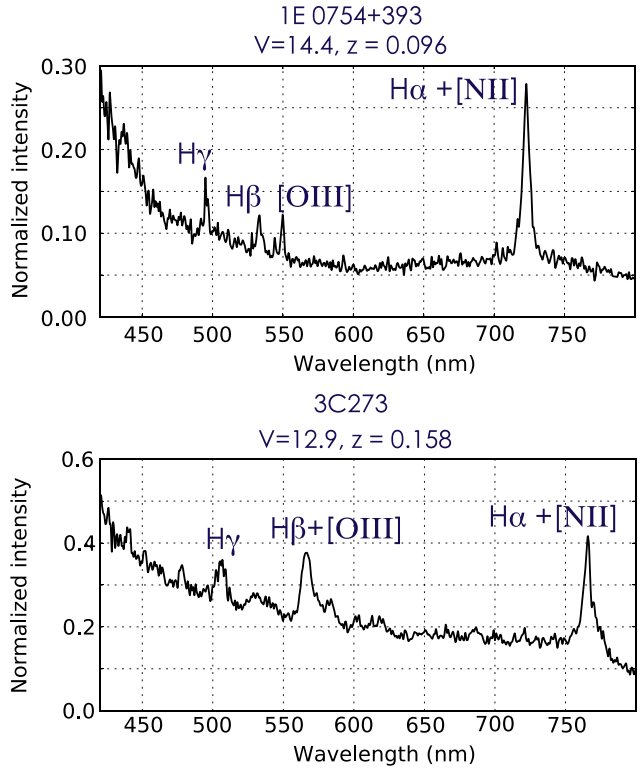

Fig. 10. CGS spectra of two low-redshift quasars, each with prominent redshifted Balmer emission lines, as well as a forbidden oxygen line. (a) 1E 0754+393,V = 14.4, z = 0.096 and (b) 3C273, $V = 12.9, z = 0.158$. Each exposure was 15 min.

velocities of these quasars using the Doppler formula and can determine distances using Hubble's law. Using the Iowa Robotic Observatory, the RMS error on the measured redshift is ∼0.002 or ∼600 km s^{-1}.

IV. LIMITATIONS

The grism system described here is slitless, so that only point sources can be observed with good spectral resolution. In principle, one could add a slit in front of the grism, but since it is in the converging light cone of the telescope, there would be substantial light loss from vignetting. Also, centering the target is critical for accurate wavelength calibration, particularly in the direction parallel to the dispersion axis. For example, with a 600 lpmm grating and a telescope with a focal length of 3 m, the wavelength displacement is about 0.5 nm/arc sec. Finally, filter wheel modification to accommodate the grism height is more difficult with some filter wheels than others. For example, some filter wheels have electronics boards that interfere with a simple housing extension modification, so users should carefully inspect their filter wheel design before deciding to incorporate a grism system.

V. ADAPTING THE CGS TO OTHER OBSERVATORIES

Details for design and construction of a compact grism system, including Winlens[22] files for the optical design and OnShape[23] files for the grism enclosure and housing extenders for several commercial filter wheels, can be found on the Iowa Robotic Telescope website. The Python scripts for

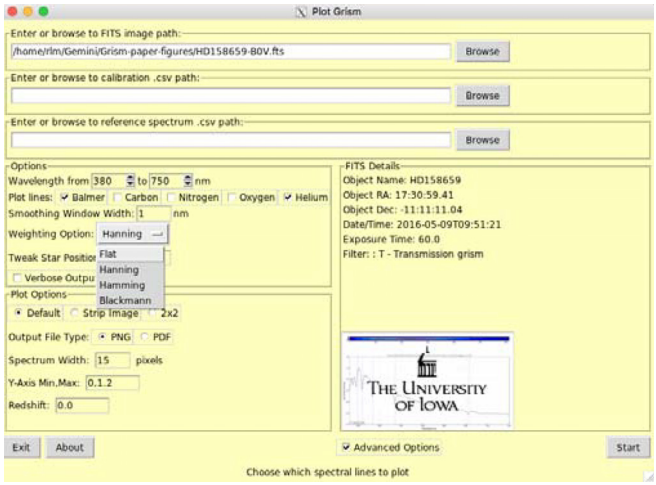

Fig. 11. Graphical user interface to the CGS calibration and plotting program designed for ease of student use.

calibration and display of CGS spectra are open-source and available on GitHub[24] and include a user-friendly GUI interface (Fig. 11).

ACKNOWLEDGMENTS

This research was partially funded by NSF Grant No. 1517152, the Carver Trust Grant No. 15-4579, and the University of Iowa College of Liberal Arts.

[a]Electronic mail: ludovici@rose-hulman.edu

[b]Electronic mail: robert-mutel@uiowa.edu

[1]E. Bardar, "Development and analysis of spectroscopic learning tools and the light and spectroscopy concept inventory for introductory college astronomy," Ph.D. thesis, Erin M. Bardar, Diss. Abstr. Int., B **67**, 2037–2228 (Boston University, MA, 2006).
[2]K. Brecher, "Do atoms really 'emit' absorption lines?," Phys. Teach. **29**, 454–456 (1991).
[3]S. Ratcliff, D. Noss, J. Dunham, E. Anthony, J. Cooley, and A. Alvarez, "High-resolution solar spectroscopy in the undergraduate physics laboratory," Am. J. Phys. **60**, 645–649 (1992).
[4]S. Ratcliff, B. Martin, A. Ambuske, R. Lu, E. Blair, S. Randall, and S., Kono, "Modular spectrographs for undergraduate laboratories," Am. J. Phys. **79**, 716–722 (2011).
[5]J. Beaver and C. Conger, "Extremely low cost point-source spectrophotometry," in *31st Annual Symposium on Telescope Science*, Society for Astronomical Sciences, 2012, pp. 112–120.
[6]J. Beaver and D. Robert, "A CCD spectrometer for one dollar," in *Earth and Space Science: Making Connections in Education and Public Outreach* (A.S.P.C., San Francisco, 2011), p. 425.
[7]"Rainbow optics star spectroscope," <http://www.starspectroscope.com/>.
[8]"Rspec star analyzer," <http://www.rspec-astro.com/star-analyser/>.
[9]R. Hood, J. Moore, M. McKinlay, D. Coffin, D. Trieweiler, and R. Mutel, *Transmission Grating Spectrometers in Undergraduate Astronomy Laboratories* (B.A.A.S., Austin, Texas, 2012).
[10]Eugene Hecht, *Optics*, 4th ed. (Addison-Wesley, San Francisco, CA, 2002), pp. 264–266.
[11]"Richardson gratings technical Note 5: GRISMS (GRATING PRISMS)," <https://www.gratinglab.com/Information/Technical_Notes/TechNote5.aspx>.
[12]"Hubble space telescope WFC3 grism," <http://www.stsci.edu/hst/wfc3/analysis/grism_obs/wfc3-grism-resources.html/>.
[13]J. Prasad, G. Mitra, and P. K. Jain, "Aberrations of a system of arbitrarily inclined planar surfaces placed in non-collimated light beam," Nouv. Rev. Opt. **6**, 345–352 (1975).
[14]"Edmund optics," <https://www.edmundoptics.com>.
[15]"Ross optical," <http://www.rossoptical.com>.

[16]"Thorlabs," <https://www.thorlabs.com>.
[17]"DC3 pinpoint," <http://pinpoint.dc3.com/>.
[18]G. Jacoby, D. Hunter, and C. Christian, "A library of stellar spectra," Astrophys. J. Suppl. Ser. **56**, 257–281 (1984).
[19]D. Silva and M. Cornell, "A new library of stellar optical spectra," Astrophys. J. Suppl. Ser. **81**, 865–881 (1992).
[20]"Iowa robotic observatory," <http:astro.physics.uiowa.edu/iro>.
[21]"Winer observatory," <http:/winer.org/>.
[22]"Winlens" <http://www.winlens.de/>.
[23]"OnShape.com," <http://www.onshape.com/>.
[24]"Github repository for grism calibration and plotting software," <https://github.com/IowaRoboticTelescope/Grism-plotter>.

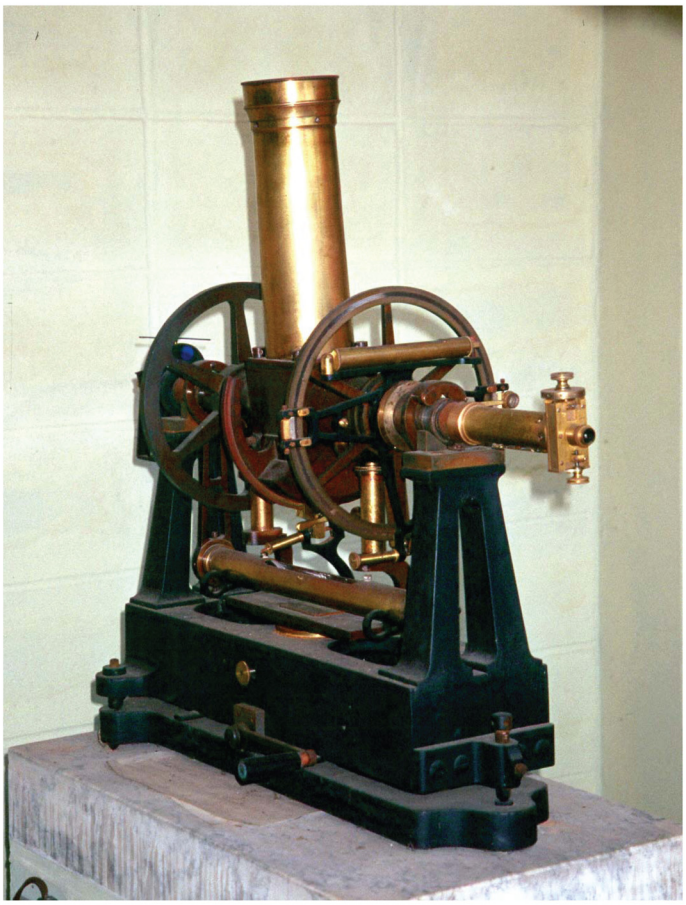

Astronomical Transit Instrument

The typical small 19th century observatory had three instruments: a refracting telescope for examining astronomical bodies, an accurate pendulum clock and a transit instrument. The latter was placed in a southward-facing window of the observatory and was aligned so that its field of view traversed the local meridian. By noting the time at which stars passed by, it was possible to determine the local time relative to Greenwich Mean Time. This example is at the Observatory of Franklin and Marshall College in Lebanon, Pennsylvania. (Picture and Notes by Thomas B. Greenslade, Jr., Kenyon College)